DALTON
FULL PAPER

Organized assemblies of lead(II) complexes of a tetraiminodiphenol macrocyclic ligand: manifestation of weak metal–anion interactions and the directional influence of anions

Bula Dutta,[a] Bibhutosh Adhikary,[b] Pradip Bag,[a] Ulrich Flörke[c] and Kamalaksha Nag*[a]

[a] *Department of Inorganic Chemistry, Indian Association for the Cultivation of Science, Jadavpur, Kolkata 700 032, India. E-mail: ickn@mahendra.iacs.res.in*
[b] *Department of Chemistry, B. E. College (A Deemed University), Howrah 711 103, India*
[c] *Anorganische und Analytische Chemie der Universität Gesamthochschule Paderborn, D-33098, Paderborn, Germany*

Received 12th February 2002, Accepted 1st May 2002
First published as an Advance Article on the web 28th May 2002

The syntheses and crystal structures of the lead(II) complexes $[Pb(LH_2)(ClO_4)][ClO_4]$, $[Pb(LH_2)(NO_3)_2]$ and $[Pb_2L(NO_3)_2]$ of the tetraiminodiphenol macrocyclic ligand (H_2L) derived from a [2+2] condensation reaction between 2,6-diformyl-4-methylphenol and 1,3-diaminopropane are reported. In the mononuclear complexes, the two uncoordinated imino nitrogens are protonated and are hydrogen bonded to the phenolate oxygens. A supramolecular assembly occurs for $[Pb(LH_2)(ClO_4)][ClO_4]$, due to weak interactions between the metal and three oxygen atoms of three different symmetry-related perchlorates, thereby forming a hexameric species with a propeller structure. $[Pb(LH_2)(NO_3)_2]$, however, is a monomer with normal bidentate binding modes for the nitrates. By contrast, $[Pb_2L(NO_3)_2]$ exhibits a 2-D structural network comprising parallel chains from two independent $[Pb_2L]^{2+}$ units, to which the nitrate anions are associated rather unconventionally: one oxygen is coordinated to two symmetry-related metal centres, another oxygen to a single lead, while the third oxygen remains free. The structural features of the complexes in solution have been investigated by ^1H NMR spectroscopy.

Introduction

Over the past three decades extensive studies have been made on the chemistry of phenolate-bridged metal complexes derived from Schiff base-type dinucleating macrocyclic ligands **I**.[1–6] The symmetric ligand **II** has been of particular interest because it provides an ideal platform for the investigation of cooperative interactions between two metal centres (the same or different) under identical stereochemical environments. The focus of interest in complexes of this sort has been the probing of magneto-structural relations,[7–14] redox activities[3,6,15–21] and selective activation of substrates.[6,22] Although a large number of these macrocyclic complexes have been structurally characterized, they are virtually all derived from divalent metal ions. Significantly, there remains, however, wider scope to study M(III)M(II), M(III)M′(II), M(III)M(III) or M(III)M′(III) types of systems. This is especially relevant in the context of modelling the active sites of non-heme iron proteins such as hemerythrine,[23] methane monooxygenase,[24] purple acid phosphatase,[25] ribonucleotide reductase[26] and calcineurin.[27]

In our efforts to develop systematically the chemistry of mixed-valent M(III)M(II), mixed-metal M(III)M′(II) and isovalent M(III)M(III) complexes of **II** (H_2L), we introduce here a core complex cation, $[Pb(LH_2)]^{2+}$ (**III**), which serves as a useful precursor for the generation of other mononuclear $[M(LH_2)]^{2+}$ and $[M(LH_2)]^{3+}$ species. The present study is concerned with the eleboration of the structural features of three lead(II) complexes, $[Pb(LH_2)(ClO_4)]_6[ClO_4]_6$, $[Pb(LH_2(NO_3)_2]$ and $[Pb_2L(NO_3)_2]_\infty$, in the solid state and in solution. It is demonstrated that the influences of weak metal–anion interactions, anion-imposed directionality and crystallographic symmetry requirements all combine together to set out the structural paradigm.

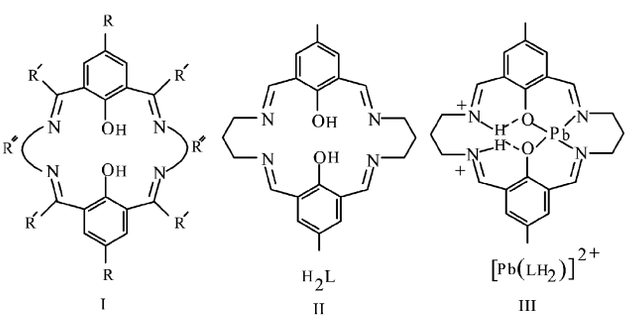

I II III

Experimental

Materials

Reagent grade chemicals obtained from commercial sources were used as received. 2,6-Diformyl-4-methylphenol was prepared according to the literature method.[16b,28]

Preparation of the complexes

CAUTION: all the perchlorate salts reported in this study are potentially explosive and therefore should be handled with care.

$[Pb(LH_2)(ClO_4)][ClO_4]$ (1). To a boiling methanol solution (100 cm^3) of 2,6-diformyl-4-methylphenol (3.28 g, 20 mmol) was added a methanol solution (20 cm^3) of $Pb(ClO_4)_2 \cdot 3H_2O$ (4.6 g, 10 mmol) and 1.5 cm^3 of acetic acid. The solution was kept stirred and 1,3-diaminopropane (1.48 g, 20 mmol) diluted with methanol (20 cm^3) was added. The color of the solution changed from light yellow to orange and, eventually, a yellow

 DOI: 10.1039/b201608g

polycrystalline product began to separate out. Refluxing of the mixture was continued for 3 h, after which it was kept at room temperature for another 3 h. The product was collected by filtration and washed with methanol and diethyl ether; yield 6.4 g (80%). Found: C, 35.6; H, 3.4; N, 6.8; $C_{24}H_{28}N_4O_2Pb(ClO_4)_2$ requires: C, 35.5; H, 3.5; N, 6.9%. Selected IR data on KBr (ν/cm^{-1}): 3440br, 3040br, 1647s, 1546s, 1460m, 1353m, 1273m, 1235m, 1092s, 1057sh, 991m, 871w, 807w, 623m, 491w. UV-vis data in DMF [λ_{max}/nm (ε/dm^3 mol^{-1} cm^{-1})]: 408 (24 000).

Crystals of **1** for structure determination were obtained in the following way. A multiple-necked round bottomed flask was fitted with three graduated pressure-equilized addition funnels, a reflux condenser and a thermometer. The flask was charged with 200 cm^3 methanol, 5 cm^3 *N*,*N*-dimethylformamide (DMF) and 0.5 cm^3 acetic acid. The reaction temperature of the bath was set to 55 °C and from the addition funnels three solutions of 0.66 g 2,6-diformyl-4-methylphenol, 0.9 g $Pb(ClO_4)_2\cdot 3H_2O$ and 0.3 g 1,3-diaminopropane each dissolved in 30 cm^3 methanol were added simultaneously at the rate of 1 cm^3 min^{-1}. The solution was kept at 55 °C for 4 h and then brought to room temperature over a period of 8 h. The crystals that deposited on the wall of the flask were collected after 24 h.

[Pb(LH$_2$)(NO$_3$)$_2$] (2). To a boiling methanol solution (60 cm^3) containing 2,6-diformyl-4-methylphenol (1.64 g, 10 mmol) and acetic acid (1 cm^3), finely ground $Pb(NO_3)_2$ (1.65 g, 5 mmol) dissolved in DMF (15 cm^3) was added, followed by a methanol solution (20 cm^3) of 1,3-diaminopropane (0.74 g, 10 mmol). After refluxing for 4 h, the product that deposited as yellow microcrystals was filtered off and washed with methanol and diethyl ether; yield 3.3 g (90%) Found: C, 39.25; H, 3.8; N, 11.2; $C_{24}H_{28}N_4O_2Pb(NO_3)_2$ requires: C, 39.15; H, 3.8; N, 11.4%. Selected IR data on KBr (ν/cm^{-1}): 3450br, 3030br, 1645s, 1541s, 1387w, 1460m, 1384s, 1360sh, 1266m, 1229m, 1021w, 986w, 865w, 803w, 494w.

Single crystals of **2** were obtained in the same way as described for **1**. However, in this case, the reaction flask contained 100 cm^3 methanol and 0.5 cm^3 acetic acid, while the addition funnels contained 0.66 g $Pb(NO_3)_2$ dissolved in a mixture of 10 cm^3 DMF and 20 cm^3 methanol, 0.66 g 2,6-diformyl-4-methylphenol in 30 cm^3 methanol and 0.3 g 1,3-diaminopropane in 30 cm^3 methanol.

[Pb$_2$L(NO$_3$)$_2$] (3). To a vigorously stirred boiling methanol solution (80 cm^3) of 2,6-diformyl-4-methylphenol (1.64 g, 10 mmol) were added successively a DMF solution (25 cm^3) of $Pb(NO_3)_2$ (3.31 g, 10 mmol) and a methanol solution (20 cm^3) of 1,3-diaminopropane (0.74 g, 10 mmol). In a few minutes, a canary-yellow compound began to deposit. Refluxing of the mixture was continued for 5 h, after which the product was filtered off and washed with methanol; yield 4.2 g (90%) Found: C, 30.85; H, 2.8; N, 8.85; $C_{24}H_{26}N_4O_2Pb_2(NO_3)_2$ requires: C, 30.6; H, 2.75; N, 8.95%. Selected IR data on KBr (ν/cm^{-1}): 1635s, 1561m, 1447m, 1384s, 1299m, 1256m, 1123m, 1064m, 806m, 501w, 468w.

To obtain single crystals of **3**, the following changes were made to the procedure adopted for **2**. The reaction flask contained 100 cm^3 methanol but no acetic acid and the addition funnels contained (i) 0.66 g $Pb(NO_3)_2$ dissolved in a mixture of 15 cm^3 DMF and 15 cm^3 methanol, (ii) 0.33 g 2,6-diformyl-4-methylphenol in 30 cm^3 methanol and (iii) 0.15 g 1,3-diaminopropane in 30 cm^3 methanol.

[Pb$_2$L(ClO$_4$)$_2$]1.5H$_2$O (4). This compound was prepared in the same way as **3**, with the difference that a methanol solution of $Pb(ClO_4)_2\cdot 3H_2O$ was used (yield 86%). Found: C, 27.6; H, 2.9; N, 5.3; $C_{24}H_{26}N_4O_2Pb_2(ClO_4)_2\cdot 1.5H_2O$ requires: C, 27.9; H, 2.7; N, 5.4%. Selected IR data on KBr (ν/cm^{-1}): 3460br, 1630s, 1561m, 1446m, 1395w, 1315m, 1256w, 1122s, 1086sh, 1064s, 803m, 620m, 501w. UV-vis data in DMF [λ_{max}/nm (ε/dm^3 mol^{-1} cm^{-1})]: 392 (32 000).

Although single crystals of **4** were obtained as before, they spontaneously lose a solvent molecule on removal from the mother liquor.

[Cd(LH$_2$)][ClO$_4$]$_2$ (5). To a boiling acetonitrile solution (50 cm^3) of **1** (0.81 g, 1 mmol) was added a solution of $CdCl_2\cdot 2.5H_2O$ (0.23 g, 1 mmol) in acetonitrile (10 cm^3). After 0.5 h, the precipitated $PbCl_2$ was removed by filtration and 0.5 g $NaClO_4$ was added to the filtrate. On concentration of the solution to *ca.* 20 cm^3, a bright yellow crystalline product was obtained, which was filtered and washed with 1 : 1 acetonitrile–methanol mixture; yield 0.43 g (60%). Found: C, 40.05; H, 4.05; N, 7.9; $C_{24}H_{28}N_4O_2Cd(ClO_4)_2$ requires: C, 40.25; H, 3.9; N, 7.85%. Selected IR data on KBr (ν/cm^{-1}): 3025br, 1645s, 1542s, 1455m, 1360m, 1273m, 1235m, 1091s, 1055sh, 996m, 917w, 877w, 811w, 625m, 566w, 497w. UV-vis data in DMF [λ_{max}/nm (ε/dm^3 mol^{-1} cm^{-1})]: 406 (21 600).

[Cd$_2$L(NO$_3$)$_2$] (6), [Zn$_2$L(NO$_3$)$_2$] (7). To a boiling methanol solution (50 cm^3) containing 2,6-diformyl-4-methylphenol (0.33 g, 2 mmol) and $Cd(NO_3)_2\cdot 6H_2O$ (0.84 g, 2 mmol) or $Zn(NO_3)_2\cdot 6H_2O$ (0.60 g, 2 mmol), a methanol solution (5 cm^3) of 1,3-diaminopropane (0.15 g, 2 mmol) was slowly added. The resulting lime solution was refluxed for 4 h, during which period the cadmium complex deposited as a greenish-yellow polycrystalline material and was separated by filtration (60%). The solution containing zinc was concentrated to *ca.* 20 cm^3 which, on standing, gave a canary-yellow crystalline product and was collected by filtration (70%).

6. (Found: C, 38.6; H, 3.6; N, 11.05. $C_{24}H_{26}N_4O_2Cd_2(NO_3)_2$ requires: C, 38.35; H, 3.45; N, 11.2%). Selected IR data on KBr (ν/cm^{-1}): 1633s, 1560s, 1464m, 1384s, 1328m, 1282m, 1235w, 1123m, 1070m, 1023w, 818m, 778w, 506w. UV-vis data in DMF [λ_{max}/nm (ε/dm^3 mol^{-1} cm^{-1})]: 380 (31 600).

7. (Found: C, 43.7; H, 4.05; N, 12.65. $C_{24}H_{26}N_4O_2Zn_2(NO_3)_2$ requires: C, 43.85; H, 3.95; N, 12.8%). Selected IR data on KBr (ν/cm^{-1}): 1636s, 1563s, 1450m, 1384s, 1328m, 1282m, 1235m, 1123m, 1070w, 818m, 771w, 512w. UV-vis data in DMF [λ_{max}/nm (ε/dm^3 mol^{-1} cm^{-1})]: 370 (17 200).

Measurements

Elemental C, H and N analyses were performed in-house on a Perkin–Elmer 2400II elemental analyzer. Infrared spectra were recorded on a FT-IR Nexus Nicolet spectrometer using KBr discs. Electronic spectra were measured in DMF on a Shimadzu UV-2100 spectrophotometer. The ^{1}H, {^{1}H–^{1}H} COSY and variable temperature NMR spectroscopic measurements were performed on a Bruker Avance DPX-300 spectrometer in $(CD_3)_2SO$ solutions.

X-Ray crystallography

Single crystals of **1**, **2** and **3** were mounted on glass fibres and coated with epoxy resin. Intensity data were collected with a Siemens R3m/V diffractometer at 203 K using graphite-monochromated Mo-Kα radiation (λ = 0.71073 Å). The cell parameters were obtained by least-squares refinement of twenty automatically centred reflections. The standard reflections were measured after every 150 observations during data collection and no significant variations in intensities were observed. Crystal data and details of structure determinations are summarized in Table 1. The intensity data were corrected for Lorentz-polarization effects and semi-empirical absorption corrections were made from Ψ-scans. The structures were solved by direct and Fourier methods and refined by full-matrix least-squares based on F^2 using the programs SHELXTL-PLUS[29] and SHELXL-93.[30] Neutral atom scattering factors were taken from Cromer and Waber.[31] The non-hydrogen atoms

Table 1 Crystallographic data for $[Pb(LH_2)(ClO_4)][ClO_4]$ (**1**), $[Pb(LH_2)(NO_3)_2]$ (**2**) and $[Pb_2L(NO_3)_2]$ (**3**)

	1	**2**	**3**
Formula	$C_{24}H_{28}Cl_2N_4O_{10}Pb$	$C_{24}H_{28}N_6O_8Pb$	$C_{24}H_{26}N_6O_8Pb_2$
M	810.59	735.71	940.89
Crystal size/mm	0.20 × 0.17 × 0.15	0.20 × 0.40 × 0.22	0.58 × 0.32 × 0.28
Crystal system	Hexagonal	Monoclinic	Triclinic
Space group	$R\bar{3}$	$P2_1/n$	$P\bar{1}$
a/Å	35.124(5)	10.277(1)	7.582(1)
b/Å	35.124(5)	17.922(3)	9.531(1)
c/Å	12.095(4)	14.368(3)	18.285(2)
α/°	—	—	95.30(1)
β/°	—	92.08(1)	91.00(1)
γ/°	120	—	92.69(1)
U/Å^3	12922(4)	2644.6(8)	1313.9(3)
Z	18	4	2
D/g cm^{-3}	1.875	1.848	2.378
T/K	203(2)	203(2)	203(2)
μ/mm^{-1}	6.122	6.439	12.858
No. measured, observed reflections	6919, 5831	7520, 6082	7234, 6010
Parameters refined	371	353	362
Final $R1$,[a] $wR2$[b] [$I > 2\sigma(I)$]	0.0748, 0.1429	0.0385, 0.0619	0.0450, 0.1060
$R1$, $wR2$ (all data):	0.2748, 0.2227	0.0703, 0.0693	0.0653, 0.1150
S[c]	0.866	0.973	1.028

[a] $R1(F) = \Sigma||F_o| - |F_c||/\Sigma|F_o|$. [b] $wR2(F^2) = [\Sigma w(F_o^2 - F_c^2)^2/\Sigma w(F_o^2)^2]^{1/2}$. [c] $S = [\Sigma w(F_o^2 - F_c^2)^2/(N - P)]^{1/2}$ where N is the number of data and P the total number of parameters refined.

were refined anisotropically, while the hydrogen atoms were placed at the geometrically calculated positions with fixed isotropic thermal parameters.

CCDC reference numbers 179593–179595.

See http://www.rsc.org/suppdata/dt/b2/b201608g/ for crystallographic data in CIF or other electronic format.

Results and discussion

Syntheses

The condensation reactions involving one equivalent each of 2,6-diformyl-4-methylphenol, 1,3-diaminopropane and lead nitrate or lead perchlorate produce the corresponding dinuclear lead complexes $[Pb_2L(NO_3)_2]$ (**3**) and $[Pb_2L(ClO_4)_2]$ (**4**) in near quantitative yield. When these reactions are carried out with half an equivalent of the metal salts, complexes **3** and **4** are again obtained, but the yields of the products are less than half those of the previous reactions. The lack of formation of the neutral lead complex [PbL] coupled with the absence of any reported $[M^{II}L]$ compound indicate the thermodynamic instability of such species, arising from the propensity to hydrolytic cleavage of the non-coordinated imine groups of the macrocycle. A useful approach to circumvent nucleophilic attack on the CH=N groups and, hence, to stabilize the mononuclear complex species would be to protonate the imine nitrogens so that they become intramolecularly hydrogen bonded with the phenolate oxygens (as shown in **III**). We have found that this can be readily achieved by carrying out the condensation reaction in the presence of a weak acid. Thus, when one equivalent of lead perchlorate or lead nitrate is reacted with two equivalents each of 2,6-diformyl-4-methylphenol and 1,3-diaminopropane, and 2–3 equivalents of acetic acid, the imine-protonated mononuclear complexes $[Pb(LH_2)(ClO_4)][ClO_4]$ (**1**) and $[Pb(LH_2)(NO_3)_2]$ (**2**) are obtained in high yield (>80%).

We note that in a study involving the reaction of equivalent amounts of 1,3-diamine-2-hydroxypropane, 2,6-diformyl-4-methylphenol and lead perchlorate in methanol, the formation of three products and their structural characterization as the dinuclear macrocyclic lead complex $[Pb_2(H_2L')][ClO_4]_2$, the nononuclear protonated complex $[Pb(H_4L')][ClO_4]_2$ and the metal-free protonated macrocyclic ligand salt $[(H_6L')(H_2O)_2][ClO_4]_2$ has been reported.[32] The dilead complex was obtained as the initial reaction product, while the other two compounds were obtained on keeping the reaction mixture for several days. Moreover, the proportion of the metal-free macrocycle was found to increase with time. Furthermore, imine-protonated mononuclear cryptates of several di- and trivalent metal ions derived from [2 + 3] condensation reaction between tris(2-aminoethyl)amine and 2,6-diformyl-4-methylphenol have been reported by others[33] using a different synthetic protocol.

Preliminary studies have shown that complexes **1** and **2** are convenient precursors for the preparation of mononuclear complexes of other metal ions which are kinetically either inert or labile in the oxidation states +2 and +3. For example, the inert complexes $[Pt(LH_2)][ClO_4]_2$ and $[Rh(LH_2)Cl(H_2O)][ClO_4]_2$, and the labile complexes $[Ga(LH_2)Cl(H_2O)][ClO_4]_2$ and $[Ln(LH_2)Cl_2(H_2O)_2][ClO_4]$ can be obtained by the metathetical reaction between **1** and the chloride salt of the required metal ion in acetonitrile. The precipitation of $PbCl_2$ acts as a driving force for the replacement reaction. The transmetallation reaction can also be carried out by using a relatively harder metal ion without recourse to precipitation of $PbCl_2$. For instance, complex **2** on treatment with an equivalent amount of the nitrate salt of a lanthanide in methanol affords the complex $[Ln(LH_2)(NO_3)_2][NO_3]$.

A characteristic feature in the IR spectra of the mononuclear complexes is the occurrence of a weak band at about 3030 cm^{-1} due to the $\nu_{N-H\cdots O}$ vibration. Moreover, the $\nu_{C=N}$ stretching vibration for the mononuclear compounds is observed at a somewhat higher energy (*ca.* 1645 cm^{-1}) relative to that for the dinuclear compounds (*ca.* 1635 cm^{-1}).

Crystal structures

$[Pb(LH_2)(ClO_4)][ClO_4]$ (1). The structural analysis of complex **1** has revealed the presence of the core cation $[Pb(LH_2)]^{2+}$ and two perchlorate anions. An ORTEP representation of the $[Pb(LH_2)]^{2+}$ cation is shown in Fig. 1 and selected interatomic distances and angles are listed in Table 2.

The lead atom occupying one of the compartments of the macrocyclic ligand is bonded to the phenolate oxygens [Pb(1)–O(1) = 2.388(14), Pb(1)–O(2) = 2.356(13) Å] and to the imine nitrogens N(1) and N(2) [Pb(1)–N(1) = 2.539(18), Pb(1)–N(2) = 2.488(17) Å]. The non-coordinated imine nitrogens N(3) and N(4) are separated from O(2) and O(1) by 2.63 and 2.57 Å, respectively. Although the hydrogen atoms connected to these two protonated imine nitrogens could not be seen, they appear to be strongly hydrogen bonded to the phenolate oxygens, with the N–H ⋯ O angles being 131.9 and 131.3°. The angles

Table 2 Selected bond lengths (Å) and angles (°) for $[Pb(LH_2)(ClO_4)][ClO_4]$ (**1**) and $[Pb(LH_2)(NO_3)_2]$ (**2**)

1		**2**	
Pb(1)–O(1)	2.388(14)	Pb(1)–O(1)	2.373(4)
Pb(1)–O(2)	2.356(13)	Pb(1)–O(2)	2.363(4)
Pb(1)–N(1)	2.539(18)	Pb(1)–N(1)	2.580(5)
Pb(1)–N(2)	2.488(17)	Pb(1)–N(2)	2.559(4)
Pb(1)–O(21A)	2.767(17)	Pb(1)–O(11)	2.831(4)
Pb(1)–O(24B)	2.972(17)	Pb(1)–O(13)	3.027(4)
Pb(1)–O(23)	3.004(17)	Pb(1)–O(21)	2.960(5)
N(3) ··· O(2)	2.63(2)	Pb(1)–O(23)	2.855(5)
N(4) ··· O(1)	2.57(2)	N(3) ··· O(2)	2.61(2)
		N(4) ··· O(1)	2.60(2)
O(1)–Pb(1)–O(2)	76.3(5)	O(1)–Pb(1)–O(2)	78.70(13)
O(2)–Pb(1)–N(2)	74.1(6)	O(2)–Pb(1)–N(2)	71.51(13)
N(2)–Pb(1)–N(1)	70.4(6)	N(2)–Pb(1)–N(1)	67.98(13)
N(1)–Pb(1)–O(1)	73.5(5)	N(1)–Pb(1)–O(1)	71.17(13)
O(1)–Pb(1)–N(2)	111.2(5)	O(1)–Pb(1)–N(2)	107.81(14)
O(2)–Pb(1)–N(1)	119.8(5)	O(2)–Pb(1)–N(1)	117.52(13)
N(3)–H(3A) ··· O(2)	132.5(2)	O(11)–Pb(1)–O(13)	43.18(11)
N(4)–H(4A) ··· O(1)	131.7(2)	O(21)–Pb(1)–O(23)	42.53(12)

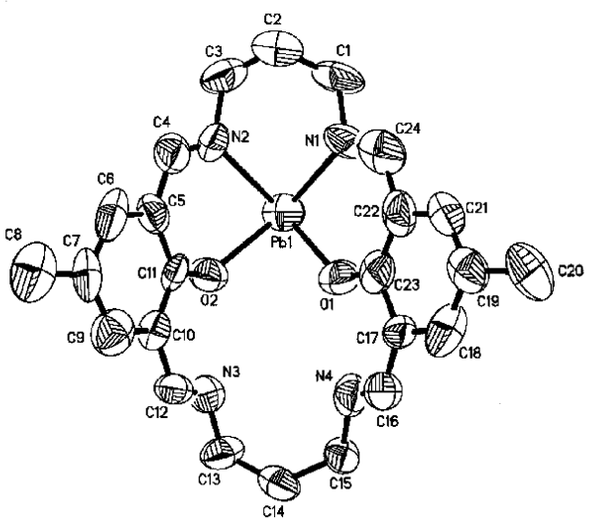

Fig. 1 ORTEP representation of the $[Pb(LH_2)]^{2+}$ cation of complex **1** at the 50% probability level.

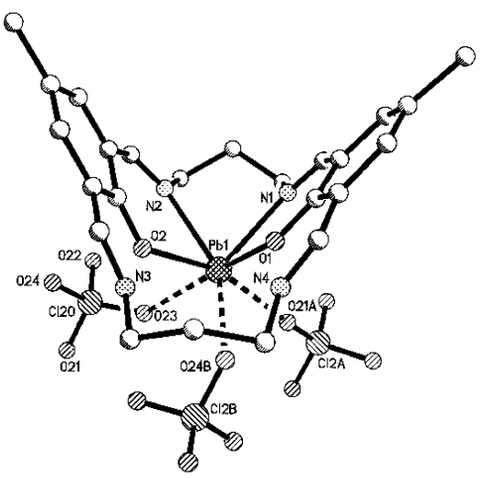

Fig. 2 The mode of linkage of the Cl(20) perchlorate ion and two other symmetry-related perchlorate ions, Cl(2A) and Cl(2B), with the core $[Pb(LH_2)]^{2+}$ cation of **1**.

involving the metal centre all deviate considerably from 90°; the angles O(1)Pb(1)O(2), N(1)Pb(1)N(2), O(1)Pb(1)N(1) and O(2)Pb(1)N(2) lie between 70.4(6) and 76.3(5)°, while the angles O(1)Pb(1)N(2) and O(2)Pb(1)N(1) are 111.2(5) and 119.8(5)°, respectively. The atoms O(1), O(2), N(1) and N(2), forming a trapezoid, are deviated from the mean plane by not more than ± 0.07 Å, while the displacement of the metal centre is 1.298(3) Å.

Of the two perchlorate ions, the one related to Cl(10) remains free. On the other hand, the oxygen atoms O(21), O(23) and O(24), but not O(22), belonging to the second perchlorate with Cl(20), weakly interact with the metal centre. The mode of binding is rather subtle in nature. Each of the three oxygen atoms are coordinated to three different but symmetrically equivalent lead units and each lead, in turn, is connected to three oxygen atoms from three different (but symmetrically equivalent) perchlorate groups, as shown in Fig. 2. The metal–anion connectivity leads to self-assembly, the course of which is governed by symmetry relationships. The process finally gives rise to supramolecular association of six $[Pb(LH_2)]^{2+}$ cations and six ClO_4^- anions. Fig. 3 shows the structure of the hexameric species $[\{Pb(LH_2)(\mu\text{-}O_3ClO)\}_6]^{6+}$ thus produced. The novel propeller-like architecture is built around a hexagonal frame provided by the lead atoms. As a result of interaction with perchlorate oxygen, the lead centre obtains a seven-fold coordination geometry in which the Pb(1)–O(21) distance

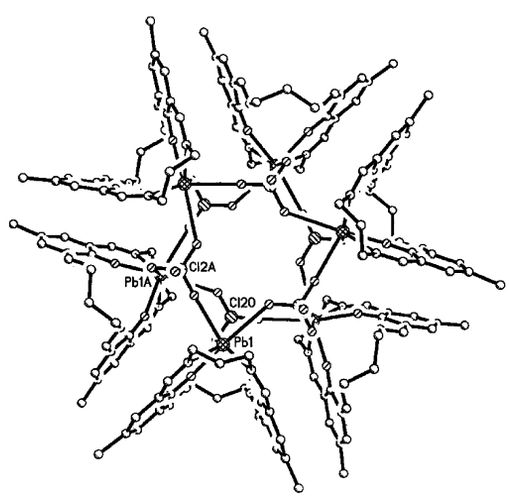

Fig. 3 A view of the self-assembled hexameric species $[\{Pb(LH_2)(ClO_4)\}_6]^{6+}$ formed for complex **1**.

[2.767(23) Å] is shorter relative to Pb(1)–O(23) [3.004(15) Å] and Pb(4)–O(24) [2.972(18) Å]. Another important consequence of this interaction is the adoption by the macrocyclic unit of a folded configuration, as is evident from the dihedral angle between the two phenyl rings of 69.3(5)°.

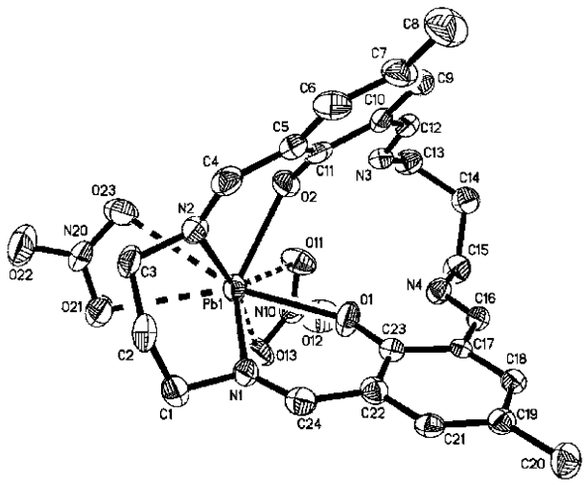

Fig. 4 ORTEP representation of $[Pb(LH_2)(NO_3)_2]$ (**2**) at the 50% probability level.

$[Pb(LH_2)(NO_3)_2]$ (2). The ORTEP representation of **2** (Fig. 4) shows that the macrocyclic ligand is bound to the metal centre in the same way as in **1**. The lead atom is additionally bound to two bidentate nitrate anions and, thus, acquires an eight-coordinate $[PbN_2O_6]$ distorted dodecahedral geometry. Table 2 lists selected bond distances and angles for **2**.

The Pb–O(phenolate) distances [av. 2.368(5) Å] and Pb–N(imine) distances [av. 2.569(9) Å] in **2** are similar to those observed in **1**. The two Pb–O distances in each of the bidentate nitrates are not identical [Pb(1)–O(11) = 2.831(4), Pb(1)–O(13) = 3.027(4); Pb(1)–O(21) = 2.960(5), Pb(1)–O(23) = 2.855 Å]. No supramolecular association occurs in **2**, presumably because of the attainment of eight-coordinate geometry by the lead. Similar to complex **1**, the protonated imines are hydrogen bonded to the adjacent phenolate oxygens [N(3) ··· O(2) = 2.61(2), N(4) ··· O(1) = 2.60(2) Å; N(3)–H(3A) ··· O(2) = 132.5(2), N(4)–N(4A) ··· O(1) = 131.7(2)°].

$[Pb_2L(NO_3)_2]$ (3). From the structural analysis of **3** it became evident that there are two halves of two independent cations per asymmetric unit and the centres of the complete $[Pb_2L(NO_3)_2]$ molecules each lie on crystallographic inversion centres. An ORTEP representation for the $[Pb_2L]^{2+}$ cation and a projection of $[Pb_2L(NO_3)_2]$ along [100] are shown in Fig. 5 and 6, respectively. Selected internuclear distances are listed in Table 3.

The macrocyclic ligand is flat in this case, the deviations of the constituent donor atoms $[N_2O_2]$ do not exceed ±0.025(5) Å

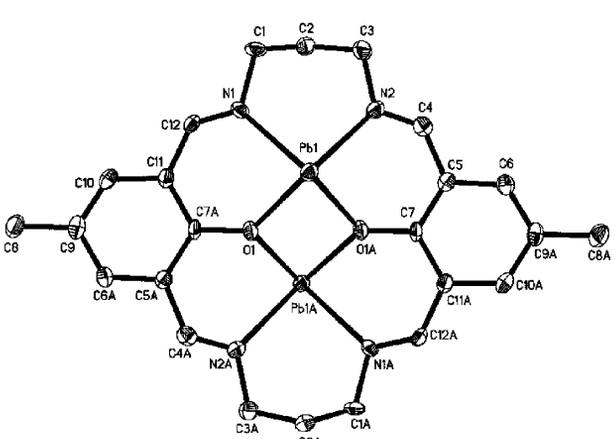

Fig. 5 ORTEP representation of the $[Pb(1)LPb(1A)]^{2+}$ cation of complex **3** at the 50% probability level. The second $[Pb(2)LPb(2A)]^{2+}$ cationic species of **3** has a similar appearence.

Table 3 Selected bond lengths (Å) and angles (°) for $[Pb_2L(NO_3)_2]$ (**3**)[a]

Pb(1)–O(1)	2.350(6)	Pb(2)–O(2)	2.355(5)
Pb(1)–O(1A)	2.366(6)	Pb(2)–O(2A)	2.357(6)
Pb(1A)–O(1)	2.366(6)	Pb(2)–O(2)	2.357(6)
Pb(1)–N(1)	2.485(7)	Pb(2)–N(3)	2.513(8)
Pb(1)–N(2)	2.567(7)	Pb(2)–N(4)	2.496(8)
Pb(1)–O(12)	2.900(7)	Pb(2)–O(22)	3.010(7)
Pb(1)–O(13)	2.962(7)	Pb(2)–O(23)	3.002(7)
Pb(1)*[b]–O(13)	3.009(7)	Pb(2)*[b]–O(23)	3.060(7)
Pb(1) ··· Pb(1A)	3.903(1)	Pb(2) ··· Pb(2A)	3.891(1)
O(1)–Pb(1)–O(1A)	68.3(2)	O(2)–Pb(2)–O(2A)	68.7(2)
O(1)–Pb(1)–N(1)	72.9(2)	O(2)–Pb(2)–N(4)	73.5(2)
O(1A)–Pb(1)–N(2)	71.7(2)	O(2A)–Pb(2)–N(3)	72.2(2)
N(1)–Pb(1)–N(2)	79.4(2)	N(3)–Pb(2)–N(4)	79.0(2)
O(1)–Pb(1)–N(2)	115.4(2)	O(2)–Pb(2)–N(3)	117.5(2)
O(1A)–Pb(1)–N(1)	113.4(2)	O(2A)–Pb(2)–N(4)	112.4(2)
Pb(1)–O(1)–Pb(1A)	111.7(2)	Pb(2)–O(2)–Pb(2A)	111.3(2)
O(12)–Pb(1)–O(13)	43.5(2)	O(23)–Pb(2)–O(23)	41.7(2)

[a] There are two independent molecules in the unit cell. [b] Metal centre belongs to another molecule related by symmetry.

from the least-squares planes. The metal centres are displaced from the basal plane in opposite direction by 1.316 Å [Pb(1)/Pb(1A)] and 1.301(1) Å [Pb(2)/Pb(2A)]. The N(10) nitrate coordinates to Pb(1)/Pb(1A) and the N(20) nitrate to Pb(2)/Pb(2A) in the same pattern, albeit the binding mode is rather uncommon. The metal centre obtains a seven-coordinate geometry due to three-fold coordination by the nitrate ions, two oxygen atoms stem from one nitrate group and the third oxygen atom stems from a second but symmetry-related nitrate group. This latter oxygen bridges two lead atoms from two different (but symmetry-related) $[Pb_2L]^{2+}$ units. Thus, one oxygen atom from each nitrate is bound to two lead atoms, another oxygen atom to one lead, while the third oxygen atom is not involved in O ··· Pb interaction (Fig. 6). As shown in Fig. 7, the whole structure then consists of parallel ··· $(NO_3)_2$ ··· $[Pb_2L]$ ··· $(NO_3)_2$ ··· $[Pb_2L]$ ··· $(NO_3)_2$ ··· chains along [010], one chain includes the crystallographic Pb(1)/Pb(1A) atoms and the other chain the Pb(2)/Pb(2A) atoms, which, viewed along [010], give rise to a two-dimensional self-assembled network.

The average Pb–O(phenolate) distance [2.357(7) Å] in **3** is very similar to that in **2** [2.368(5) Å], however, the corresponding Pb–N(imine) distances [2.52(4) Å for **3** and 2.57(1) Å for **2**] are not so close. The Pb–O(nitrate) distances in the two sets of $[Pb_2L(NO_3)_2]$ are not exactly identical. The distances involving Pb(1)–O(12), Pb(1)–O(13) and the symmetry-related Pb(1)*–O(13) bond are 2.900(7), 2.962(7) and 3.009(8) Å, respectively, and may be compared with the corresponding distances involving Pb(2)–O(22) [3.017(7) Å], Pb(2)–O(23) [3.022(7) Å] and Pb(2)*–O(23) [3.060(9) Å]. The non-bonded metal–metal distance is 3.903(1) Å for Pb(1A) ··· Pb(1A) and 3.891(1) Å for Pb(2) ··· Pb(2A). On the other hand, the separations between the planes of the macrocycles $[Pb_2L]$ ··· $[Pb_2L]$ are 4.106(2) Å [involving Pb(1)/Pb(1A)] and 4.139(2) Å [involving Pb(2)/Pb(2A)].

^{1}H NMR spectroscopy

Proton NMR spectroscopic studies were carried out for complexes **1**–**7** in dimethyl sulfoxide and the observed chemical shifts are listed in Table 4. The spectral assignments (Table 4) were facilitated by ^{1}H–^{1}H correlation spectroscopy (COSY). The mononuclear lead complexes **1** and **2** exhibit identical spectra, as do the dinuclear complexes **3** and **4**, indicating that, in dimethyl sulfoxide, solvation of the core complex cation leads to complete dissociation of the anions.

The spectral features exhibited by the mononuclear lead (**1**, **2**) and cadmium (**5**) complexes are quite similar in the lower field region. For example, the hydrogen-bonded protonated imine $^+$N–H ··· O (**a**, proton labelling scheme is shown in

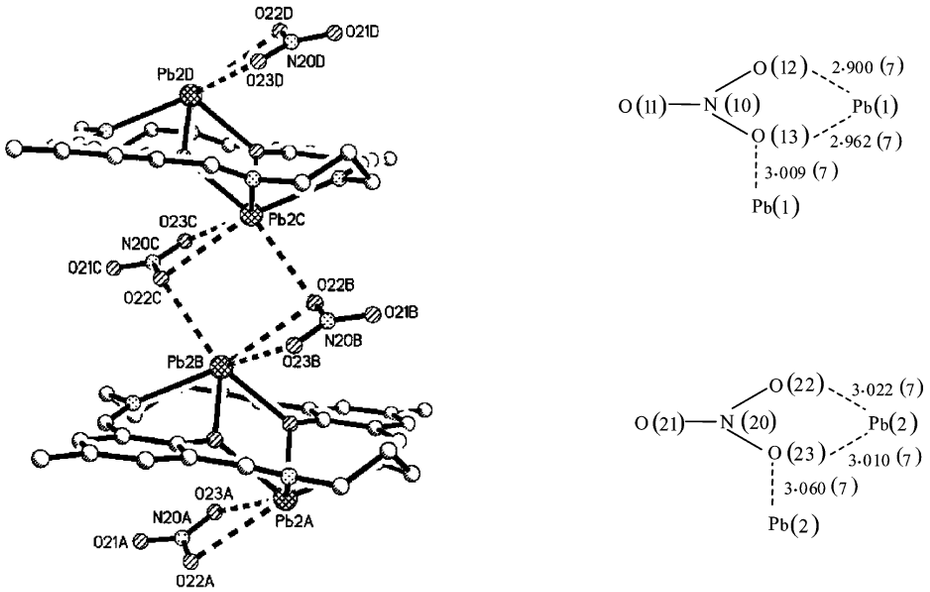

Fig. 6 The binding mode of the nitrate ions in $[Pb(2)LPb(2A)(NO_3)_2]$ (**3**). The self-assembled chain is viewed along [100]. Similar chain is also formed in $[Pb(1)LPb(1A)(NO_3)_2]$.

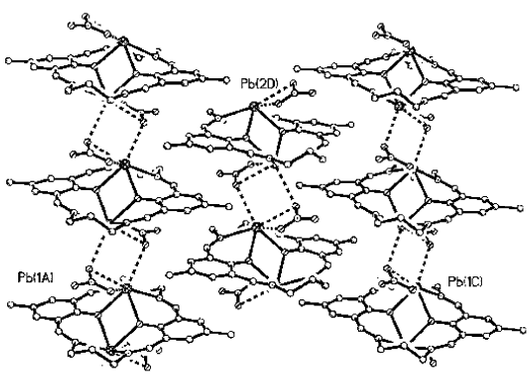

Fig. 7 A view of the 2D network along [010] for complex **3**. The alternating parallel chains consist of crystallographic Pb(1)/Pb(1A) and Pb(2)/Pb(2b) atoms.

Table 4) is observed as a broad singlet at 13.21 ppm for **1** and 13.37 ppm for **5**. Similar to complex **1**, which exhibits a doublet at 8.65 ppm (J = 13.7 Hz) and three singlets at 8.44, 7.47 and 7.36 ppm (all integrating to two protons each), complex **5** exhibits these bands at 8.63 (J = 13.2 Hz), 8.24, 7.47 and 7.30 ppm. The COSY spectra showed correlation between the doublet (**c**) and $^{+}$N–H ··· O (**a**), indicating that *trans* coupling between the NH and CH protons at the metal-free compartment causes splitting of the CH resonance to a doublet. The complimentary CH resonance (**b**) at the metal-containing part is associated with weak satellites due to S = 1/2 metal isotopes. Thus, the singlet at 8.44 ppm for complex **1** has satellite peaks due to ^{207}Pb (J = 25 Hz), while for complex **5**, the peak at 8.24 ppm shows satellites due to ^{111,113}Cd (J = 30 Hz). Of the two aromatic protons (**d** and **e**), the less shielded resonance seems to be due to the one closer to the protonated imine. In the aliphatic region, although the chemical shift due to CH_3 (**f**) is almost identical for **1** (2.16 ppm) and **5** (2.17 ppm), significant differences are observed in the two cases for the CH_2 resonances. Thus, while for complex **1** five signals at 4.24 (2), 3.94 (4), 3.77 (2), 2.39 (2) and 1.48 (2) ppm are observed (values in parentheses indicate the number of protons), only two signals at 3.93 (8) and 2.23 (4) are observed for complex **5**. The COSY spectrum of **1** showed correlation between the following pairs: 3.94 and 13.21, 3.94 and 2.39, and 4.24 and 1.58. Taken together, it may be concluded that while the $CH_2CH_2CH_2$ protons on the Pb side are anisochronous and are observed at 4.24 (**g**) and 3.77 (**h**) ppm, they are isochronous on the metal-free side (**i** = **j**, 3.94 ppm). The $CH_2CH_2CH_2$ protons on both the sides, however, are isotropic, and the one in the vicinity of Pb is more shielded. In complex **5**, no anisotropic effect is observed and the equivalence of the $CH_2CH_2CH_2$ and $CH_2CH_2CH_2$ protons on both the sides appears to be accidental.

The effect of variation of temperature (25 to 70 °C) on the resonances of complex **1** is shown in Fig. 8. As can be seen, the doublet (**b**) and the singlet (**c**) due to the imino CH approach

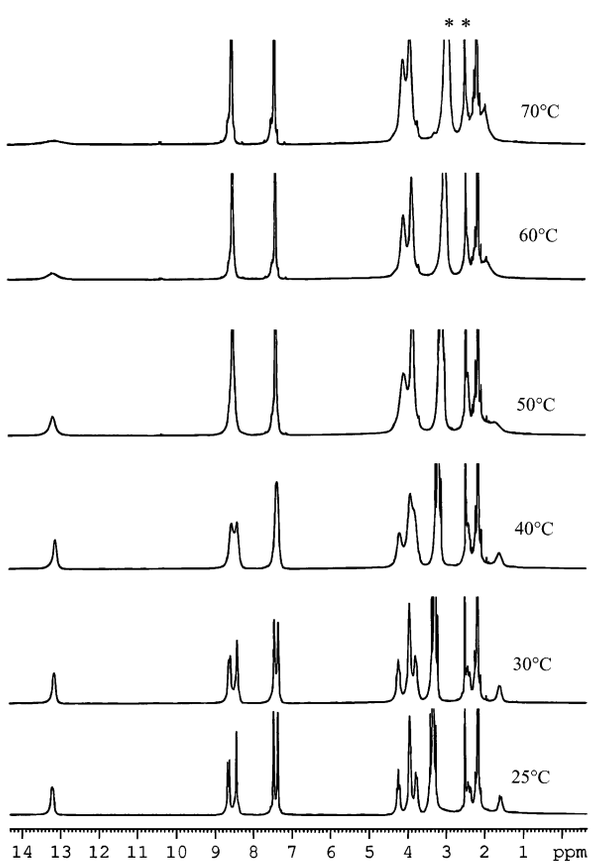

Fig. 8 ^{1}H NMR spectra at different temperatures for the $[Pb(LH_2)]^{2+}$ cation of **1** in $(CD_3)_2SO$. The peaks due to the solvent and HOD are marked with asterisks.

Table 4 Proton NMR spectra of complexes **1**–**7**[a]

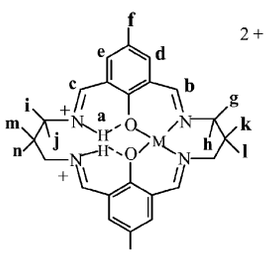

1 , 2 , 5

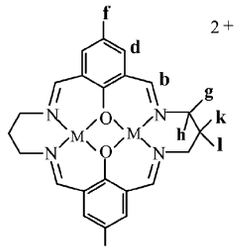

3 , 4 , 6 , 7

Assignment		$[Pb(LH_2)]^{2+}$ **1**, **2**	$[Cd(LH_2)]^{2+}$ **5**	$[Pb_2L]^{2+}$ **3**, **4**	$[Cd_2L]^{2+}$ **6**	$[Zn_2L]^{2+}$ **7**
N^+–H ··· O	**a**	13.21 (s, 2)	13.37 (s, 2)			
HN^+=CH	**b**	8.44 (s, 2)[b]	8.24 (s, 2)[c]	8.43 (s, 4)[d]	8.36 (s, 4)[e]	8.49 (s, 4)
	c	8.65 (d, 2)	8.63 (d,2)			
Aromatic	**d**	7.36 (s, 2)	7.30 (s, 2)	7.36 (s, 4)	7.34 (s, 4)	7.52 (s, 4)
	e	7.47 (s, 2)	7.47 (s, 2)			
CH_3	**f**	2.16 (s, 6)	2.17 (s, 6)	2.29 (s, 6)	2.24 (s, 6)	2.28 (s, 6)
CH_2	**g**	4.24 (t, 2)	3.93 (m, 8)	4.37 (t, 4)	3.92 (m, 8)	3.97 (m, 8)
	h	3.77 (d, 2)		3.86 (dd, 4)		
	i	3.94 (d, 4)				
	j	—	—	—	—	—
	k	1.58 (q, 2)	2.23 (m, 4)	1.66 (q, 4)	1.99 (m, 4)	1.94 (m, 4)
	l	—	—	—	—	—
	m	2.39 (m, 2)				
	n	—	—	—	—	—

[a] Spin multiplicity and the number of protons are given in parenthesis. [b] ^{207}Pb satellites, J = 25 Hz. [c] ^{111,113}Cd satellites, J = 30 Hz. [d] ^{207}Pb satellites, J = 22 Hz. [e] ^{111,113}Cd satellites, J = 20 Hz.

each other and coalesce at 50 °C, while the chemical shifts due to the aromatic singlets (**d** and **e**) get averaged at 40 °C. Significant changes occur for the signals due to the CH_2 protons, with increasing temperature, the rotational barriers for the **g** and **h** protons decrease, and they collapse at *ca.* 60 °C. Variation of the temperature produces little effect on the chemical shifts due to the CH_3 (**f**) and N–H ··· O (**a**) moieties. Over the increasing temperature range (25 to 70 °C, the chemical shift of **f** changes from 2.16 to 2.18 ppm, while for **a**, the change from 13.21 to 13.17 ppm is accompanied by a considerable increase in line broadening.

The dinuclear lead (**3**, **4**) and cadmium(**6**) complexes display well-resolved satellite peaks due to the coupling of ^{207}Pb–CH (**b**) [J = 22 Hz] and ^{111,113}Cd–CH(**b**) [J = 20 Hz]. Similar to their mononuclear analogues, complexes **4** and **6** differ with regard to the CH_2 resonances. Complex **4** exhibits three signals at 4.37, 3.86 and 1.66 ppm, each arising from four protons. Complex **6**, as well as the dizinc complex **7**, however, show only two resonances, from eight and four protons [**6**: 3.92(8) and 1.99(4); **7**: 3.97(8) and 1.94(4) ppm], due to the $CH_2CH_2CH_2$ and $CH_2CH_2CH_2$ protons, respectively. The COSY spectrum of **4** showed that the resonance at 4.37 ppm is correlated with the resonances at 3.86 and 1.66 ppm, indicating anisochronous behaviour of these $CH_2CH_2CH_2$ protons. Clearly, free rotation of CHH′ in the vicinity of the larger Pb^{2+} ion (vdW r = 1.19 Å) is more restricted relative to Cd^{2+} (0.95 Å) and Zn^{2+} (0.74 Å).

It would be of interest to compare such parameters as the chemical shift due to $^+$N–H ··· O and the *trans* coupling between $^+$N–H and C–H for the mononuclear lead (**1**, **2**) and cadmium (**5**) complexes with similar mononuclear metal cryptates.[33] For the divalent metal ion cryptates, the following δ and J values for these parametrs have been reported:[33] Pb^{2+} (13.59 ppm,13.5 Hz), Cd^{2+} (13.84 ppm, 13.6 Hz), Zn^{2+} (13.86 ppm, 13.6 Hz) and Ca^{2+} (13.53 ppm, 14.1 Hz). The corresponding values observed for **1** (13.21 ppm, 13.7 Hz) and **5** (13.37 ppm, 13.2 Hz) are quite similar.

A second point of interest in this context would be to compare the magnitude of the satellite coupling to Pb or Cd isotopes in the mononuclear *vis-à-vis* dinuclear complexes. In the case of the mononuclear cadmium complex **5**, J = 30 Hz, while for the dinuclear cadmium compound **6**, the J value (20 Hz) is considerably less. Such a difference in J values, however, is not so conspicuous between the mononuclear and dinuclear lead complexes **1** (25 Hz) and **3** (22 Hz).

Conclusion

A convenient synthetic route to obtain the mononuclear macrocyclic lead complexes $[Pb(LH_2)(ClO_4)][ClO_4]$ and $[Pb(LH_2)(NO_3)_2]$ of the type **III** has been developed. These compounds can be readily converted to other $[M(LH_2)]^{n+}$ (n = 2, 3) complex species, which, in turn, could be used as precursors for synthesizing various heterometallic and heterovalent complexes of the symmetrical tetraiminodiphenol macrocyclic ligand **II**. It has been observed that the solid state architectures obtained for $[Pb(LH_2)(ClO_4)][ClO_4]$ and $[Pb_2L(NO_3)_2]$ owe their origin to weak interactions between the metal cation and the anions, the dentacity and directionality of the anions and crystallographic symmetry requirements. Thus, $[Pb(LH_2)(ClO_4)][ClO_4]$ assembles to a hexameric species through three-fold coordination of the perchlorate ion, in which the metal atoms of the macrocyclic units are arranged around a hexagonal frame like butterflies. A different type of chain structure develops for $[Pb_2L(NO_3)_2]$ *via* an uncommon bridging binding mode of the nitrate ions. In solution, the ^{1}H NMR spectra show considerable differences in the number and patterns of resonances due to the methylene protons for both mononuclear and dinuclear lead complexes as compared to their cadmium and zinc analogues. In the lead complexes, the CHH′ protons in the vicinity of the metal atoms are anisochronous, while they are isochronous in the cadmium and zinc complexes, thereby showing the considerable influence of the size of the metal ions on the rotational barrier of the CH_2 groups.

References

1 N. H. Pilkington and R. Robson, *Aust. J. Chem.*, 1970, **23**, 2225.
2 S. E. Groh, *Isr. J. Chem.*, 1976/77, **15**, 277.
3 P. Zanello, S. Tamburini, P. L. Vigato and G. A. Mazzocchin, *Coord. Chem. Rev.*, 1987, **77**, 165.
4 A. J. Atkins, D. Black, A. J. Blake, A. Marin-Becerra, S. Parsons, L. Ruiz-Ramirez and M. Schroder, *Chem. Commun.*, 1996, 457.
5 H. Okawa, H. Furutachi and D. E. Fenton, *Coord. Chem. Rev.*, 1998, **174**, 51.
6 B. Bosnich, *Inorg. Chem.*, 1999, **38**, 2554.
7 (*a*) S. L. Lambert and D. N. Hendrickson, *Inorg. Chem.*, 1979, **18**, 2683; (*b*) C. L. Spiro, S. L. Lambert, T. J. Smith, E. N. Duesler, R. R. Gagne and D. N. Hendrickson, *Inorg. Chem.*, 1981, **20**, 1229; (*c*) S. L. Lambert, C. L. Spiro, R. R. Gagne and D. N. Hendrickson, *Inorg. Chem.*, 1982, **21**, 68.
8 P. Lacroix, O. Kahn, F. Theobald, J. Le Roy and C. Wakselman, *Inorg. Chim. Acta*, 1988, **142**, 129.
9 (*a*) S. K. Mandal, L. K. Thompson and K. Nag, *Inorg. Chim. Acta*, 1988, **149**, 247; (*b*) S. K. Mandal, L. K. Thompson, M. J. Newlands, E. J. Gabe and K. Nag, *Inorg. Chem.*, 1990, **29**, 1324.
10 L. K. Thompson, S. K. Mandal, S. S. Tanclon, J. N. Bridson and M. K. Park, *Inorg. Chem.*, 1996, **35**, 3317, and references cited therein.
11 K. Brychy, K. Dräger, K.-J. Jeans, M. Tilset and U. Behrnes, *Chem. Ber.*, 1994, **127**, 465.
12 S. Mohanta, B. Adhikary, S. Baitalik and K. Nag, *New J. Chem.*, 2001, **25**, 1466.
13 (*a*) H.-R. Chang, S. K. Larsen, P. D. W. Boyd, C. G. Pierpont and D. N. Hendrickson, *J. Am. Chem. Soc.*, 1988, **110**, 4565; (*b*) D. Luneau, J.-M. Savariault, P. Cassoux and J.-P. Tuchagues, *J. Chem. Soc., Dalton Trans.*, 1988, 1225.
14 (*a*) H. Sakiyama, H. Okawa and M. Suzuki, *J. Chem. Soc., Dalton Trans.*, 1993, 3823; (*b*) C. Higuchi, H. Sakiyama, H. Okawa, R. Isobe and D. E. Fenton, *J. Chem. Soc., Dalton Trans.*, 1994, 1097.
15 (*a*) A. W. Addison, *J. Inorg. Nucl. Chem. Lett.*, 1976, **12**, 899; (*b*) K. K. Nanda, A. W. Addison, N. Paterson, E. Sinn, L. K. Thompson and U. Sakaguchi, *Inorg. Chem.*, 1998, **37**, 1028.
16 (*a*) R. R. Gagne, C. A. Koval, T. J. Smith and M. C. Cimolino, *J. Am. Chem. Soc.*, 1979, **101**, 4571; (*b*) R. R. Gagne, C. L. Spiro, T. J. Smith, C. A. Hamann, W. R. Thies and A. K. Shiemke, *J. Am. Chem. Soc.*, 1981, **103**, 4073.
17 R. C. Long and D. N. Hendrickson, *J. Am. Chem. Soc.*, 1983, **105**, 1513.
18 (*a*) S. K. Mandal and K. Nag, *J. Chem. Soc., Dalton Trans.*, 1983, 2429; (*b*) S. K. Mandal, B. Adhikary and K. Nag, *J. Chem. Soc., Dalton Trans.*, 1986, 1175; (*c*) S. K. Mandal, L. K. Thompson, K. Nag, J.-P. Charland and E. J. Gabe, *Inorg. Chem.*, 1987, **26**, 1391; (*d*) S. K. Mandal, L. K. Thompson, M. J. Newlands and E. J. Gabe, *Inorg. Chem.*, 1989, **28**, 3707.
19 (*a*) R. Das, K. K. Nanda, I. Paul, S. Baitalik and K. Nag, *Polyhedron*, 1994, **13**, 2639; (*b*) S. Mohanta, S. Baitalik, S. K. Dutta and B. Adhikary, *Polyhedron*, 1998, **17**, 2669.
20 M. P. Suh, H. K. Kim, M. J. Kim and K. Y. Oh, *Inorg. Chem.*, 1992, **31**, 3620.
21 (*a*) H. Wada, T. Aono, K. Motoda, M. Ohba, N. Matsumoto and H. Okawa, *Inorg. Chim. Acta*, 1996, **246**, 13; (*b*) T. Aono, H. Wada, M. Yonemura, M. Ohba, H. Okawa and D. E. Fenton, *J. Chem. Soc., Dalton Trans.*, 1977, 1527; (*c*) T. Aono, H. Wada, M. Yonemura, H. Furutachi, M. Ohba and H. Okawa, *J. Chem. Soc., Dalton Trans.*, 1997, 3029.
22 H. Furutachi, S. Fujinami, M. Suzuki and H. Okawa, *J. Chem. Soc., Dalton Trans.*, 1999, 2197, and references cited therein.
23 (*a*) M. A. Holmes and R. E. Stenkamp, *J. Mol. Biol.*, 1991, **220**, 723; (*b*) P. C. Wilkins and R. G. Wilkins, *Coord. Chem. Rev.*, 1987, **79**, 195.
24 M. Merkx, D. A. Kopp, M. H. Sazinsky, J. L. Blazyk, J. Müller and S. J. Lippard, *Angew. Chem., Int. Ed.*, 2001, **40**, 2782.
25 (*a*) T. Klabunde and B. Krebs, *Struct. Bonding (Berlin)*, 1997, **89**, 177; (*b*) J. B. Vincent, G. L. Olivier-Lilley and B. A. Averill, *Chem. Rev.*, 1990, **90**, 1447.
26 P. Nordlund and H. Eklund, *J. Mol. Biol.*, 1993, **232**, 123.
27 C. R. Kissinger, H. E. Parge, D. R. Knighton, C. T. Lewis, L. A. Pelletier, A. Tempczyk, V. J. Kalish, K. D. Tucker, R. E. Showalter, E. W. Moomaw, L. N. Gastinel, N. Habuka, X. Chen, F. Maldonado, J. E. Barker, R. Bacquet and J. E. Villafranca, *Nature*, 1995, **378**, 641.
28 F. Ulemann and K. Brittner, *Chem. Ber.*, 1909, **42**, 2539.
29 G. M. Sheldrick, SHELXTL PLUS Program Package (PC Version), University of Göttingen, Germany, 1989.
30 G. M. Sheldrick, SHELXL 93, A Program for Crystal Structure Refinement (Gamma-Test Version), University of Göttingen, Germany, 1993.
31 D. T. Cromer and J. T. Waber, *International Tables for X-Ray Crystallography*, Kynoch Press, Birmingham, 1974, vol. 4.
32 S. S. Tandon and V. McKee, *J. Chem. Soc., Dalton Trans*, 1989, 19.
33 (*a*) M. G. B. Drew, O. W. Howarth, G. G. Morgan and J. Nelson, *J. Chem. Soc., Dalton Trans.*, 1994, 3149; (*b*) M. G. B. Drew, O. W. Howarth, C. J. Harding, N. Martin and J. Nelson, *J. Chem. Soc., Chem. Commun.*, 1995, 903; (*c*) M. G. B. Drew, C. J. Harding, V. McKee, G. G. Morgan and J. Nelson, *J. Chem. Soc., Chem. Commun.*, 1995, 1035; (*d*) M. G. B. Drew, O. W. Howarth, N. Martin, G. Morgan and J. Nelson, *J. Chem. Soc., Dalton Trans.*, 2000, 1275.